Cep55 regulates embryonic growth and development by promoting Akt stability in zebrafish

Jessie Jeffery,* Christine Neyt,† Wade Moore,‡ Scott Paterson,† Neil I. Bower,† Georgia Chenevix-Trench,§ Heather Verkade,‡,1 Benjamin M. Hogan,† and Kum Kum Khanna*,2

*Signal Transduction Laboratory, QIMR Berghofer Medical Research Institute, Brisbane, Queensland, Australia; †Vascular Biology and Development Laboratory, Institute for Molecular Bioscience, The University of Queensland, Brisbane, Queensland, Australia; ‡Zebrafish Developmental Genetics Laboratory, Monash University, Clayton, Victoria, Australia; and §Cancer Genetics Laboratory, QIMR Berghofer Medical Research Institute, Brisbane, Queensland, Australia

ABSTRACT **CEP55 was initially described as a centrosome- and midbody-associated protein and a key mediator of cytokinesis. More recently, it has been implicated in PI3K/AKT pathway activation *via* an interaction with the catalytic subunit of PI3K. However, its role in embryonic development is unknown. Here we describe a *cep55* nonsense mutant zebrafish with which we can study the *in vivo* physiologic role of Cep55. Homozygous mutants underwent extensive apoptosis by 24 hours postfertilization (hpf) concomitant with cell cycle defects, and heterozygous carriers were indistinguishable from their wild-type siblings. A similar phenotype was also observed in zebrafish injected with a *cep55* morpholino, suggesting the mutant is a *cep55* loss-of-function model. Further analysis revealed that Akt was destabilized in the homozygous mutants, which partially phenocopied Akt1 and Akt2 knockdown. Expression of either constitutively activated PIK3CA or AKT1 could partially rescue the homozygous mutants. Consistent with a role for Cep55 in regulation of Akt stability, treatment with proteasome inhibitor, MG132, partially rescued the homozygous mutants. Taken together, these results provide the first description of Cep55 in development and underline the importance of Cep55 in the regulation of Pi3k/Akt pathway and in particular Akt stability.—Jeffery, J., Neyt, C., Moore, W., Paterson, S., Bower, N. I., Chenevix-Trench, G., Verkade, H., Hogan, B. M., Khanna, K. K. Cep55 regulates embryonic growth and development by promoting Akt stability in zebrafish. *FASEB J.* 29, 1999–2009 (2015). www.fasebj.org**

Key Words: apoptosis · PI3K/AKT pathway · cytokinesis · multinucleation

CEP55 WAS INITIALLY IDENTIFIED as a centrosomal protein that localizes to the midbody during cytokinesis (1). It has since been shown to localize to the mitotic spindle and central spindle during mitosis and has microtubule-bundling activity (2, 3). CEP55 is phosphorylated on serine 425 and serine 428 by cyclin-dependent kinase 1/extracellular signal-related kinase (CDK1/ERK) upon mitotic entry, which allows it to bind the peptidyl-propyl isomerase, PIN1 (1, 4). These events prime CEP55 for polo-like kinase 1 (PLK1) binding, which phosphorylates it on serine 436 (1). These phosphorylation events are not required for CEP55 localization at the midbody. Rather, PLK1 phosphorylation prevents the premature recruitment of CEP55 to the midbody (5). Phosphorylation of CEP55 during mitosis promotes its stabilization (1, 6). In fact, CEP55 is negatively regulated by p53 through the suppression of PLK1 expression (7).

CEP55 recruits a number of proteins to the midbody during cytokinesis including ALG-2-interacting protein X (ALIX), tumor suppressor gene 101 (TSG101), and members of the endosomal sorting complex required for transport (ESCRT) to promote abscission, the final stage of cytokinesis (8–10). The ability of CEP55 to recruit these proteins is mediated by the breast cancer susceptibility gene 2 (BRCA2) (11). Cells depleted of or overexpressing CEP55 exhibit multinucleation due to a failure to resolve the cytokinetic bridge, revealing a critical role for the protein in this process (1).

More recently, CEP55 has been identified as being required for the degradation of midbody remnants *via* autophagy, which occurs postcytokinesis (12, 13). Midbody remnants are targeted for degradation by the interaction of CEP55 with the autophagy receptor, neighbour of BRCA1 gene 1 (NBR1). Both CEP55 depletion and overexpression perturbs this interaction, resulting in the accumulation of midbody remnants, which is associated with both stemness and tumorigenicity. Additionally, CEP55 is also required for an alternative form of midbody removal known as midbody release (14).

Abbreviations: ALIX, ALG-2-interacting protein X; BRCA2, breast cancer susceptibility gene 2; CDK1, cyclin-dependent kinase 1; CHX, cycloheximide; ENU, N-ethyl-N-nitrosourea; ERK, extracellular signal-related kinase; ESCRT, endosomal sorting complex required for transport; FACS, fluorescence-activated cell sorting; H&E, hematoxylin and eosin; hpf, hours

(*continued on next page*)

[1] Current affiliation: Department of Biochemistry and Molecular Biology, The University of Melbourne, Melbourne, VIC, Australia.

[2] Correspondence: Signal Transduction Laboratory, QIMR Berghofer Medical Research Institute, 300 Herston Rd., Brisbane, QLD, Australia. E-mail: kumkum.khanna@qimrberghofer.edu.au

doi: 10.1096/fj.14-265090

This article includes supplemental data. Please visit *http://www.fasebj.org* to obtain this information.

CEP55 has also been reported to promote PI3K signaling. First evidence of this came with the report that CEP55 interacts with PIK3CA (also known as p110α), the catalytic subunit of PI3K (15). CEP55 overexpression stabilized PIK3CA, resulting in increased PI3K activity as well as AKT activation. CEP55 expression is upregulated by treatment with VEGF-A, resulting in stimulation of the PI3K pathway (16).

Given the numerous roles of CEP55 in growth and development, it is not surprising that CEP55 expression is dysregulated in cancer. CEP55 overexpression has been found in multiple cancers including those of the breast, liver, thyroid, and colon, where it is associated with advanced disease and metastasis (15, 17–19). CEP55 has also been identified in signatures for poor prognosis (18, 19).

Here we present the first description of a whole organism model with a *cep55* mutation. Zebrafish *cep55* is ubiquitously expressed, with highest expression in the gonads. *cep55* is maternally deposited and expressed throughout the brain and spinal cord at 24 hpf. We characterized a *cep55* mutant zebrafish with a premature stop codon resulting in a predicted functional knockout. We find that *Cep55* homozygous mutants exhibit cell death and disorganization in the brain at 24 hpf, with hydrocephaly and edema visible later. Analysis of the 24 hpf embryos revealed that although some cell cycle dysregulation occurs, the most striking aspect of this phenotype is the extensive apoptosis occurring in these embryos. Analysis of Akt and Erk signaling pathways revealed that Akt is destabilized in *cep55* mutants. We show that treatment with the proteasome inhibitor, MG132 or injection of constitutively active *myr-hPIK3CA* or *myr-mAkt1* partially rescue the dramatic embryonic phenotype. Our study highlights a novel developmental mechanism by which Cep55 regulation of Akt stability controls developmental apoptosis and is essential for early embryogenesis.

MATERIALS AND METHODS

Zebrafish maintenance and procedures

Zebrafish were kept under standard conditions as described previously (20). *cep55* heterozygous mutants (allele designation e48) were obtained through the Zebrafish Mutation Project (21). Experiments were performed in accordance with ethical guidelines and under approval from animal ethics committees at the University of Queensland, QIMR Berghofer Medical Research Institute and The School of Biologic Sciences, Monash University.

Zebrafish were genotyped for *cep55* mutation by amplifying a 600 bp fragment using forward (5′-TGGTGTTTCTAAACGAAGACAA-3′) and reverse (5′-CTTTGATAGTCATTGGCTGCT-3′) primers then sequencing the fragment using the forward primer and Big Dye 3.1 sequencing mix (Life Technologies, Carlsbad, CA, USA).

Quantitative PCR

RNA was extracted by RNEasy Mini Kit or AllPrep RNA/DNA Mini Kit (Qiagen, Venlo, Limburg, Netherlands) and cDNA prepared using SuperScript III First-Strand Synthesis System (Life Technologies) according to manufacturer's directions. Quantitative PCR was performed on a LightCycler 480 (Roche, Basel, Switzerland) using SYBR Green (Roche) and the following primers: *cep55* forward (5′-GAAGGCCAGAGACCAGATCA-3′) and reverse (5′-GGGGTAAGATGCACCACAGT-3′); *p53* forward (5′-CCCATCCTCACAATCATCACT-3′) and reverse (5′-CACGCACCTCAAAAGACCTC-3′); *akt1* forward (5′-TGCACTCCGAAAGAAACGTG-3′) and reverse (5′-CGCACGACCGTAATCATTGT-3′); *akt2* forward (5′- GAGATCAGCGTCGTCAGAGA-3′) and reverse (5′-AAAAGTGTTTGGCCGAGGTC-3′); *elavl3* forward (5′-GTCAGAAAGACATGGAGCAGTTG-3′) and reverse (5′-GAACCGAATGAAACCTACCCC-3′); *glut1* forward (5′-GTGATTGGGTCCTTGCAGTT-3′) and reverse (5′-CTG- AGAAGGAGCCGAGAATG-3′); *ngn1* forward (5′-CGCACACGGATGATGAAGACTCGCG-3′) and reverse (5′-CGGTTCTTCTTCACGACGTGCACAGTGG-3′); β *2actin* forward (5′- CGAGCTGTCTTCCCATCCA-3′) and reverse (5′- TCACCAACGTAGCTGTCTTTCTG-3′); *EF1*α forward (5′-CCAAGGAAGTCAGCGCATAC-3′) and reverse (5′-CCTCCTTGCGCTCAATCTTC-3′). Transcripts were normalized against β *2Actin* or *EF1*α expression.

Constructs

cep55 sequence was amplified using the following primers: forward (5′-CCCAAGCTTACCATGGCGGCGAAGGGGGAAAGG-3′) and reverse (5′-GGGGAATTCTTAGGTGAAGCAGTAGTCGAGGTGTGC-3′). The PCR product was digested with *EcoRI* and *HindIII* then cloned into pcs2+. Antisense RNA was transcribed from DNA digested with *Not1* using the mMESSAGE mMACHINE SP6 Kit (Ambion, Life Technologies). *In situ* hybridization was performed as described previously (22).

All morpholinos were obtained from GeneTools. The following sequences were used: standard MO (5′-CCTCTTACCTCAGTTACAATTTATA-3′), *cep55* MO (5′-CAGACTTCTCGAGGTGAATTAGTCGC-3′), *p53* MO (5′-GCGCCATTGCTTTGCAAGAATTG-3′).

For rescue experiments, *pLNCX-myr-mAkt1* (#17245) and *pBABE-puro-HA-myr-hPIK3CA* (#12523) constructs were purchased from Addgene (Cambridge, MA, USA). *myr-Akt1* was amplified with Kozak sequence and *ClaI/StuI* sites using Akt1 forward (5′-ATATATCGATACCATGGGGAGCAGCAAGAGCAAGCCCAAG-3′) and reverse (5′-ATATAGGCCTTCAGGCTGTGCCACTGGC-3′) primers. *myr-PIK3CA* was amplified with Kozak sequence and *ClaI/XbaI* sites using PIK3CA forward (5′-ATATATCGATACCATGGGGTCTTCAAAATCTAAACCAAAG-3′) and reverse (5′-ATATTCTAGATCAGTTCAATGCATGCTGTTTAA-3′) primers. Digested transcripts were cloned into pcs2+. The plasmids were then digested with *Not1* and capped mRNA transcribed with the mMESSAGE mMACHINE SP6 Kit (Ambion).

Embryos were injected with morpholinos or mRNAs at the 1-cell to 2-cell stage.

Acridine orange

Protocol based on Tucker and Lardelli (23). Embryos (24 hpf) were dechorionated and stained for apoptotic cells with acridine orange in a working solution of 5 μg/ml dissolved in E3 medium for 30 minutes in the dark at 28.5°C. Stained embryos were then repeatedly washed in E3 before being anesthetized, mounted in 3% low melting temperature agarose dissolved in E3 medium and imaged on a Nikon (Chiyoda, Tokyo, Japan) C1 Upright microscope.

Fluorescence-activated cell sorting

Pools of embryos were disaggregated, stained with propidium iodide as previously described (24), and analyzed using a LSRII

(*continued from previous page*)

postfertilization; myr, myristoylated; NBR1, neighbour of BRCA1 gene 1; PLK1, polo-like kinase 1; PBST, phosphate buffered saline solution with Tween; PHH3, phospho-histone [^{3}H] serine 10; TSG101, tumor suppressor gene 101

flow cytometer (BD Biosciences, San Jose, CA, USA). Quantitative analysis and cell cycle profiling was performed using FlowJo v10 (Ashland, OR, USA).

Histology

Embryos were fixed in 2% paraformaldehyde, encased in agarose, then embedded in paraffin blocks, and 1 μm thick sections were stained with hematoxylin and eosin for histologic examination. Slides were scanned on an Aperio (Amcor, Hawthorn, VIC, Australia) ScanScope XT Slide Scanner and the images analyzed using Image Scope software (Leica, Solms, Germany).

Antibodies and reagents

The following antibodies and reagents were used: CoxIV (926-42214) (LiCor, Lincoln, NE, USA); AKT S473 (4060), AKT (4691); phospho ERK1/2 (4370), ERK1/2 (9107), cleaved Caspase-3 (9664) (Cell Signaling, Danvers, MA, USA); Actin (612656) (BD Biosciences); Acridine Orange (A1301) (Life Technologies); phosphohistone [^{3}H] serine 10 (PHH3) (06-570) (Millipore, Billerica, MA, USA); MG132 (S2619) (Selleck Chemicals, Houston, TX, USA); cycloheximide (CHX) (C4859) (Sigma-Aldrich, St. Louis, MO, USA).

Western blotting

Zebrafish were incubated in Ringer's solution pH 7.0 (58 mM NaCl, 4 mM KCl, 4.8 mM sodium hydrogen carbonate) for 10 min on ice then deyolked by washing embryos twice in Ringer's solution containing (1% PMSF, 4× protease inhibitor cocktail, 1× phosphatase inhibitor cocktail, 1 mM EDTA) and snap frozen until use. Embryos were homogenized in RIPA buffer (50 mM Tris-HCl pH 7.4, 150 mM NaCl, 1% NP-40, 0.25% sodium deoxycholate, 1 mM PMSF, 1× protease inhibitor cocktail, 1× phosphatase inhibitor cocktail). Western blotting was performed as described previously (25) except that IRDye-conjugated secondary antibodies were used and the signal detected using the Odyssey Classic scanner (LiCor).

Immunofluorescence

Embryos were fixed overnight in 2% paraformaldehyde in PBS, washed in PBS and blocked for 30 minutes with 3% bovine serum albumin in PBS. Primary antibody was diluted in blocking solution and incubated overnight at 4°C, washed thoroughly with phosphate buffered saline solution with Tween (PBST) then secondary antibody was diluted in blocking solution and incubated overnight at 4°C and washed thoroughly with PBST. Imaging was performed on a Zeiss (Oberkochen, Germany) 780 inverted microscope.

Statistical analysis

Quantitative PCR was analyzed by 2-tailed Student's *t* test. Cross-tabulations were analyzed using Fisher's exact test.

RESULTS

Characterization of zebrafish Cep55 (ZfCep55)

Bioinformatic analysis (26, 27) of zebrafish Cep55 (GenBank NP_001018598.1) revealed that it is 436 amino acids long and shares 36% identity with hCEP55 (GenBank AAH08947). hCEP55 is phosphorylated on serines 425 and 428 by CDK1/ERK, which primes it for phosphorylation by Plk1 on serine 436 (1) (**Fig. 1*A***, marked in blue). The PLK1 phosphorylation site is conserved in ZfCep55 (serine 407), as is the first of the 2 CDK1/ERK phosphorylation sites (serine 396). It is worth noting that whereas the second CDK1/ERK site is a lysine (399) in ZfCep55, there is another serine (398) adjacent to it, which may act as the second CDK1/ERK phosphorylation site.

To determine its pattern of expression in zebrafish, quantitative PCR was performed on a number of adult tissues. This revealed that *cep55* is most highly expressed in both the testes and ova (Fig. 1*B*). High levels of *cep55* were also detected in the muscle, with low levels of expression detected in other tissues. We also investigated the expression of *cep55* during embryonic development. *cep55* expression was highest at the 2-cell stage, with a dramatic decrease in levels over the following 24 hours (Fig. 1*C*). This suggests that *cep55* is maternally deposited. *cep55* expression was consistently detected at low levels after 24 hpf. *cep55* expression was further characterized by conducting *in situ* hybridization on 24 hpf embryos. This revealed that *cep55* is expressed throughout the head and spinal cord at 24 hpf (Fig. 1*D*).

Zfcep55 mutants exhibit gross morphologic defects during development

To functionally characterize the role of Cep55 during embryonic development, we obtained a zebrafish line through the Zebrafish Mutation Project that had been generated by N-ethyl-N-nitrosourea (ENU) mutagenesis. The allele e48 line contained a C115T mutation in *cep55*, resulting in the mutation of a glutamic acid to a stop codon at residue 39 (Fig. 1*A*, marked in red).

The heterozygous mutants obtained were both viable and fertile (**Fig. 2*A, B***). When 2 heterozygotes were crossed, we were unable to distinguish the heterozygous mutants from their wild-type siblings. In contrast, we observed that mutant offspring (~25%) exhibited cell death in the brain and eye at 24 hpf (Fig. 2*A*, *B*). This suggests the *cep55^{e48}* mutation is inherited in a Mendelian fashion and the phenotype is recessive.

The homozygous mutant phenotype progressed to edema, small eye, and jaw malformation at 48 and 72 hpf. Defects were also visible in the gut, swim bladder, and tail folds. The phenotype progressed to larval lethality, with homozygous mutants dying at an average of 5–7 days. A similar phenotype was also observed in zebrafish injected with a *cep55* morpholino (Supplemental Fig. 1), suggesting that the mutant is a *cep55* loss-of-function model. Unfortunately, none of the CEP55 antibodies tested cross-reacted with ZfCep55, so we were unable to confirm loss of protein product by Western blotting.

To further analyze the defect in homozygous mutants, 24 hpf embryos were fixed, embedded in paraffin and transversely sectioned, then analyzed by hematoxylin and eosin (H&E) staining. Although the gross morphologic organization was present in homozygous mutants, they exhibited a striking lack of cellularity compared with siblings (Fig. 2*C*). This indicated that the mutants were likely to have abnormal proliferation and/or apoptosis.

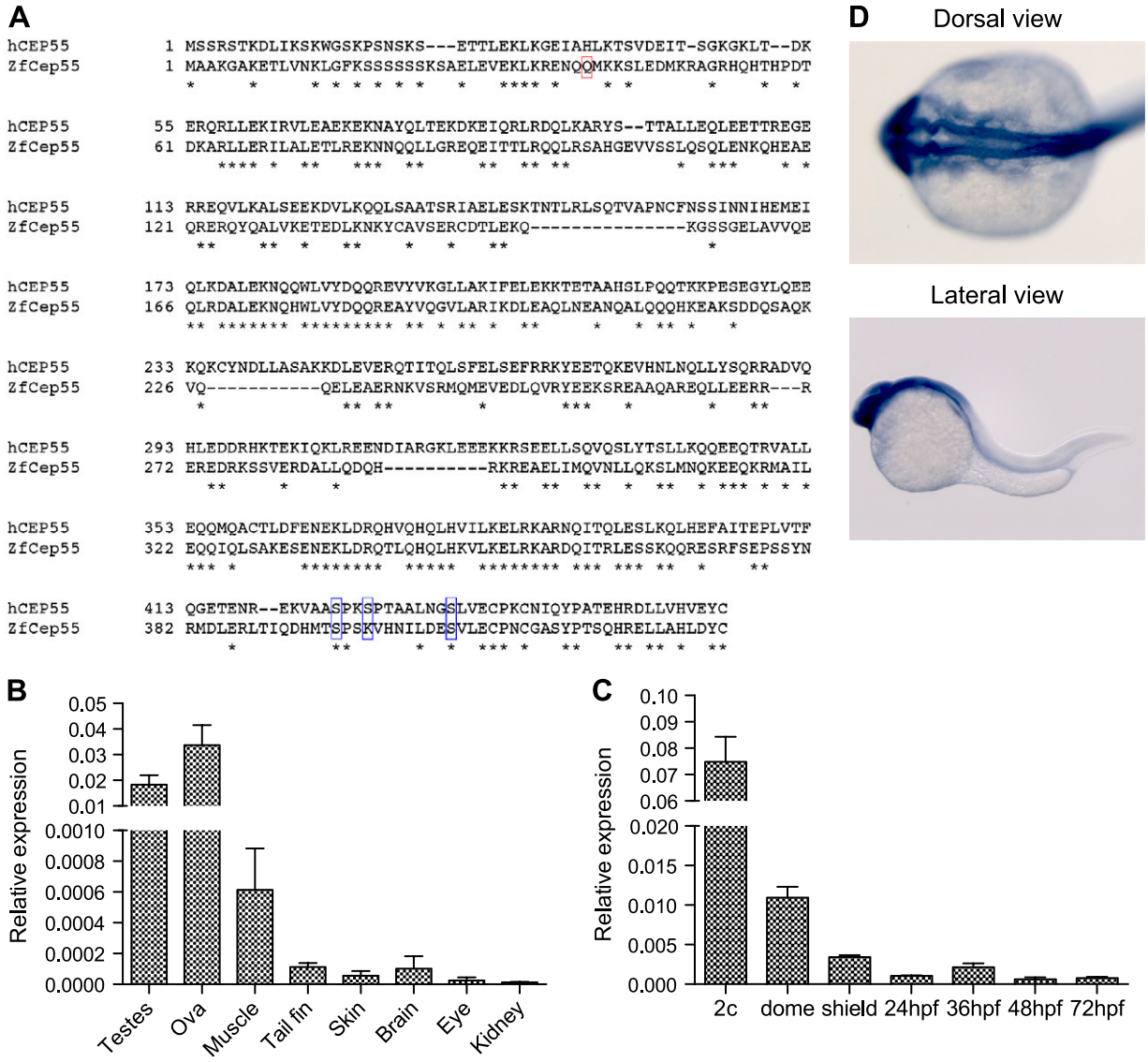

Figure 1. Characterization of *Zfcep55*. *A*) Sequence alignment of hCEP55 and ZfCep55. Residues in blue boxes indicate phosphorylation sites known to modulate hCEP55 function. Residue in red box indicates site of premature stop codon in *Zfcep55* mutants. *B*) *cep55* expression in adult tissues as measured by quantitative PCR. *C*) *cep55* expression during embryonic development as measured by quantitative PCR. 2c, 2-cell stage. *D*) *In situ* hybridization of *cep55* in 24 hpf embryos.

cep55 homozygous mutants undergo extensive apoptosis and cell cycle dysregulation

To analyze the role of Cep55 in cell cycle progression, homozygous mutant and sibling zebrafish were analyzed by fluorescence-activated cell sorting (FACS) at 24 hpf. Consistent with previous reports (28), some apoptosis was observed in sibling embryos, which displayed a sub-G1 peak containing 14.1% of cells (**Fig. 3*A***). In contrast, 50.6% of cells comprised the sub-G1 peak in homozygous mutants.

To demonstrate that homozygous mutants were undergoing extensive apoptosis, sibling and mutant embryos were stained with acridine orange, a marker that identifies dying and apoptotic cells (23). The standardized intensity of acridine orange staining in the forebrain and midbrain of mutants was 2.2 fold higher than siblings (Fig. 3*B*, *C*), further indicating that the mutant zebrafish were undergoing apoptosis. Death was confirmed to occur *via* an apoptotic pathway by staining with cleaved (activated) Caspase-3 (Supplemental Fig. 2). Apoptosis was unable to be rescued by *p53* knockdown with a previously validated morpholino (29) (Fig. 3*D*; **Table 1**).

To determine if the apoptosis was accompanied by cell cycle defects, the sub-G1 fraction was gated out and only viable cells were analyzed. This revealed a decrease in the G1 population accompanied by a 1.5-2 fold increase in S phase, G2/M phase, and >4N (aneuploid) cells (Fig. 3*E*; **Table 2**). To analyze this further, cells were stained for PHH3, a marker of cells in mitosis, but no significant differences were found (Fig 3*F*, *G*).

Pik3ca and Akt stability defects in cep55 homozygous mutants

Although human CEP55 is known to be required for cytokinesis, the phenotype of *cep55* mutant embryos was

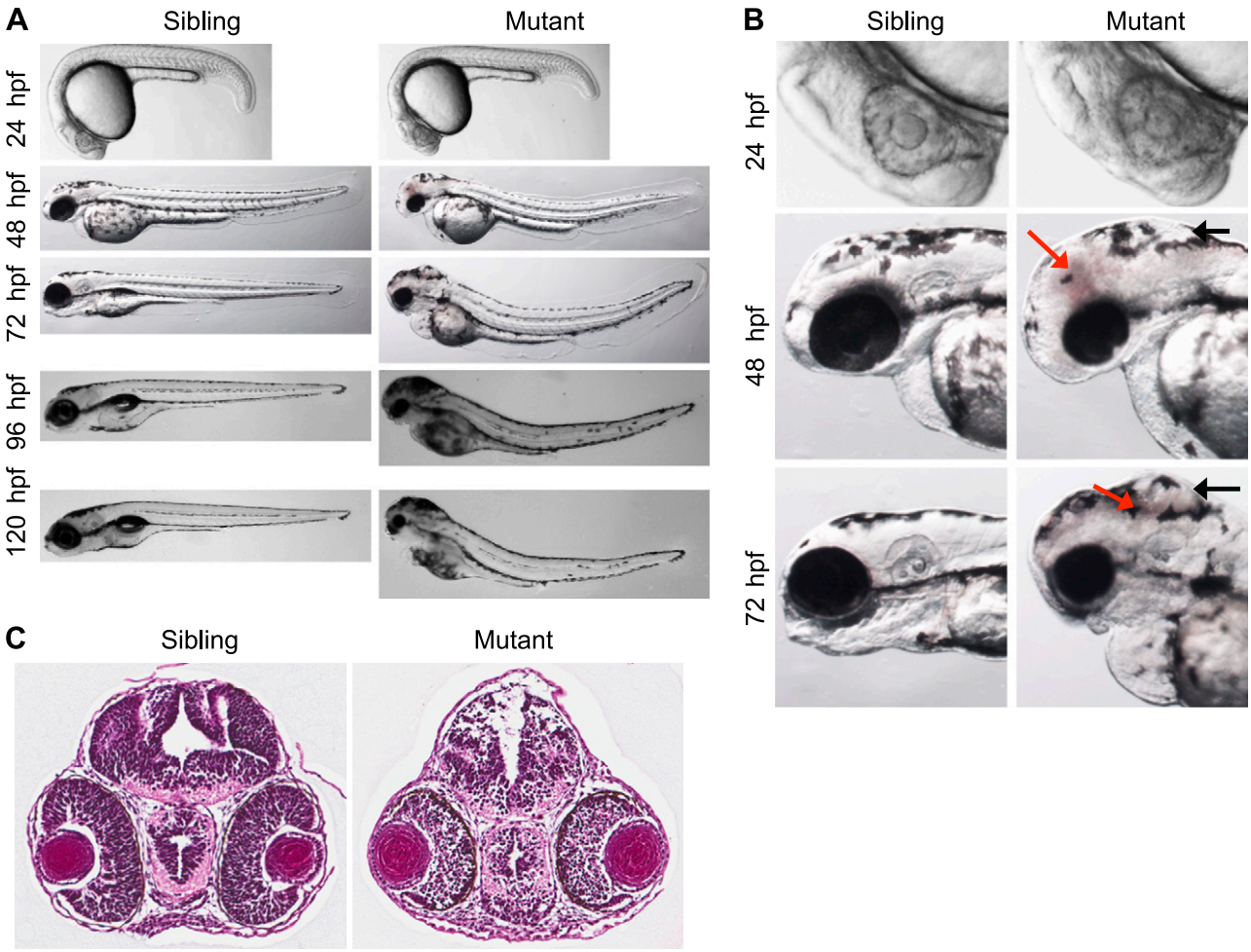

Figure 2. *cep55* homozygous mutants exhibit multiple defects. *A*) Bright-field images of homozygous mutant and sibling embryos at the indicated times. *B*) High-resolution image of head region from images in (*A*). Black arrows indicate hydrocephaly, red arrows indicate edema. *C*) Transverse sections through the eyes and brain of 24 hpf homozygous mutant and sibling embryos stained with H&E.

unable to be explained by this, as the predominant phenotype was increased apoptosis and not cytokinesis failure. In contrast, the PI3K/AKT pathway is known to promote both cell growth and survival (30). As CEP55 has been previously reported to activate the PI3K/AKT pathway by stabilizing the PI3K catalytic subunit PIK3CA (15), we hypothesized that Pi3k/Akt signaling may be perturbed in *cep55* homozygous mutants due to destabilization of Pik3ca.

Although cross-reacting PIK3CA antibodies were unavailable, we were able to measure Akt signaling as a readout of Pi3k activity. Surprisingly, total Akt protein levels were severely depleted in homozygous mutants at 24 hpf (**Fig. 4*A***). Akt activation as marked by Akt S473 phosphorylation was also reduced, but only mildly and not in line with the reduction of total protein levels, possibly indicating that the remaining Akt is hyperactivated to compensate for the depletion. In contrast, Erk1/2 signaling was not perturbed.

There are 3 zebrafish Akt genes: *akt1*, *akt2*, and *akt3*. At 24 hpf, *akt1* is expressed in the developing brain and nervous system (31). Furthermore, *akt1* knockdown by morpholino injection was reported to result in increased apoptosis as well as neuronal defects characterized by a decrease in neuronal progenitors and an increase in differentiated neurons at 24 hpf. Similarly, *akt2* knockdown resulted in increased apoptosis within 24 hpf, but this was due to a defect in glucose metabolism (32). *akt3* knockdown has not been reported in zebrafish but it is not expressed at 24 hpf (33) and therefore not physiologically relevant to the observed phenotype.

Given that the antibodies used to detect total and phosphorylated Akt recognize all Akt gene products, we investigated the distinct roles of Akt1 and Akt2 in the *cep55* mutant phenotype. Firstly, we confirmed that transcription of *akt1* and *akt2* was unperturbed in the *cep55* mutants (Fig. 4*B*, *C*).

To confirm that Akt levels were reduced due to a protein stability defect, we performed a CHX chase. Embryos at 24 hpf were treated with CHX for 0, 3, or 6 h. This revealed that Akt has a half-life of 4.7 h in sibling embryos compared with 2.0 h in homozygous mutants (Fig. 4*D*).

akt1 knockdown has been reported to result in increased neuronal differentiation concomitant with a decrease in neuronal progenitors, observed as an increase in differentiated neuron marker, *elavl3* (encodes HuC), and a decrease in neuronal progenitor marker, *ngn1* (31). Therefore, we compared *elavl3* and *ngn1* levels in *cep55* homozygous mutants with their siblings. Consistent with the decrease in Akt observed by Western blot, we observed a significant increase in *elavl3* expression and significant decrease in *ngn1* expression (Fig. 4*E*, F). Interestingly, the magnitude of

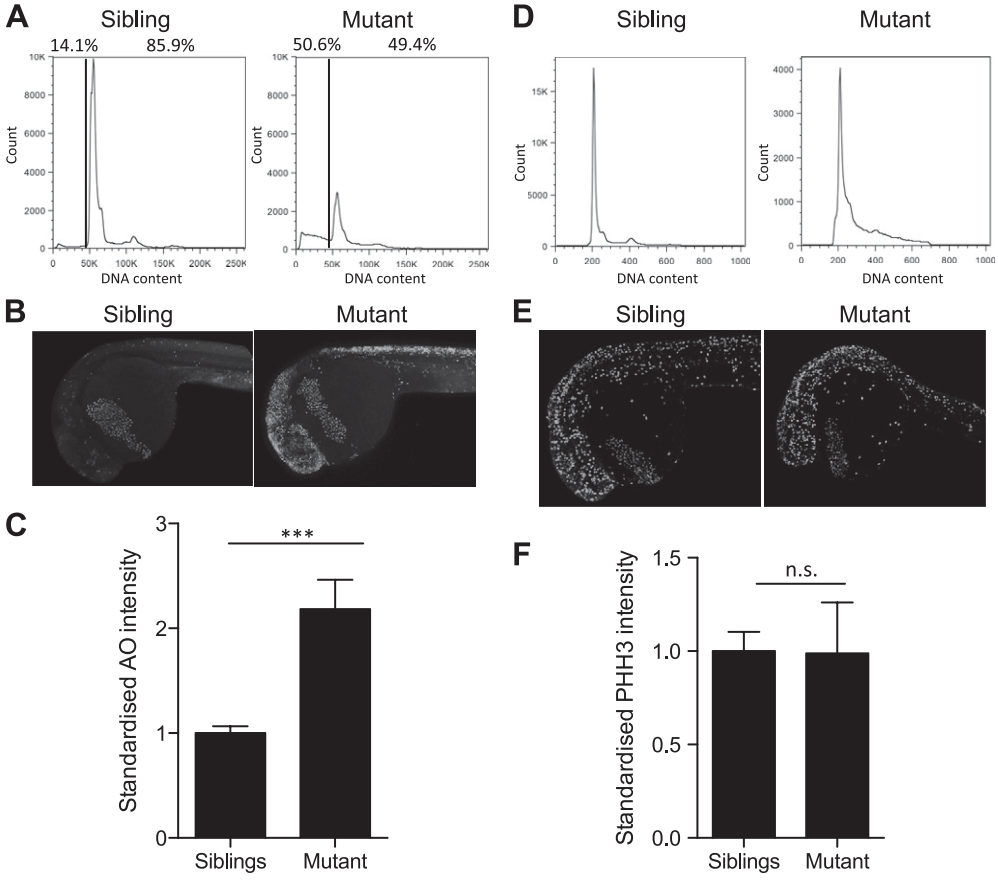

Figure 3. *cep55* homozygous mutants exhibit apoptosis and cell cycle defects. Homozygous mutant and sibling 24 hpf embryos were analyzed by FACS (*A*, *E*) or immunofluorescence (*B*, *C*, *F*, *G*). *A*) FACS analysis of sibling and mutant embryos. B) Representative images of AO staining of sibling and mutant embryos. *C*) Relative intensity of acridine orange staining from (*B*). *D*) Embryos were either uninjected or injected with p53 MO. At 24 hpf the embryos were assessed for rescue as determined by gross morphology and AO staining. *E*) FACS analysis of sibling and mutant embryos with sub-G1 population gated out. *F*) Representative images of PHH3 staining of sibling and mutant embryos. *G*) Average number of PHH3-positive cells per zebrafish embryo from *F*. Error bars represent SEM from 5 zebrafish. AO, acridine orange; MO, morpholino; n.s., not significant. ***$P < 0.001$.

increase/decrease was not as large as that documented previously in Akt1 morphant embryos (31), which is likely due to *cep55* mutants retaining some Akt activity.

Akt2 regulates glucose metabolism by promoting expression of the glucose transporter gene, *glut1*, whose expression is down-regulated in *akt2* morphant embryos (32). Therefore, we compared *glut1* expression in homozygous mutants with their siblings and found a significant decrease in its expression (Fig. 4G). Consistent with our observations in Fig. 4*E*, *F*, the magnitude of the decrease was not as large as that observed previously in *akt2* morphant embryos (32).

Constitutively active PIK3CA and AKT1 as well as proteasome inhibitor, MG132, partially rescue the cep55 homozygous mutant phenotype

To further confirm that the Pi3k-Akt pathway is perturbed in *cep55* mutant zebrafish, we examined whether constitutively active myristoylated (*myr*)-*mAkt1* or *myr-hPIK3CA* could rescue the phenotype observed in homozygous mutants. These proteins are highly conserved with 88% identity between mAKT1 and ZfAkt1 and 92% identity between hPIK3CA and the predicted ZfPik3ca. Furthermore, overexpression of mammalian AKT1 has previously been shown to phenocopy *Zfptenb* knockdown (34) and has also been used to rescue motility defects and axonal phenotypes in *Zfrgs4* knockdown zebrafish with deficient Akt signaling (35). Together, this suggests that the PI3K/AKT pathway may be functionally conserved between mammals and zebrafish.

Initially, *myr-Akt1* and *myr-PIK3CA* were titrated to determine the amount of injected mRNA that gave optimal rescue without producing any phenotype due to their overexpression. This indicated that the optimal dosages were 20 pg for *myr-Akt1* and 200 pg for *myr-PIK3CA*. Following this, embryos were split into 3 groups: uninjected,

TABLE 1. *Percentage of population in each phase of the cell cycle*

Cell cycle stage	Sibling (%)	Mutant (%)
G1	79.5	63.9
S	7.6	17.0
G2/M	10.4	14.5
>4N	2.5	4.6

TABLE 2. *Percent rescue by p53 morpholino as determined by gross morphology and AO staining*

Phenotype rescue	Uninjected	*p53* MO
Fish (*n*)	171	157
Expected ratio mutants to siblings	43 (128)	39 (118)
Necrotic eyes per brain		
n	42	40
%	24.6	25.5
% Rescue	0	−0.9
AO+ve		
n	42	38
%	24.6	24.2
% Rescue	0	0.4

AO, acridine orange; MO, morpholino; +ve, positive.

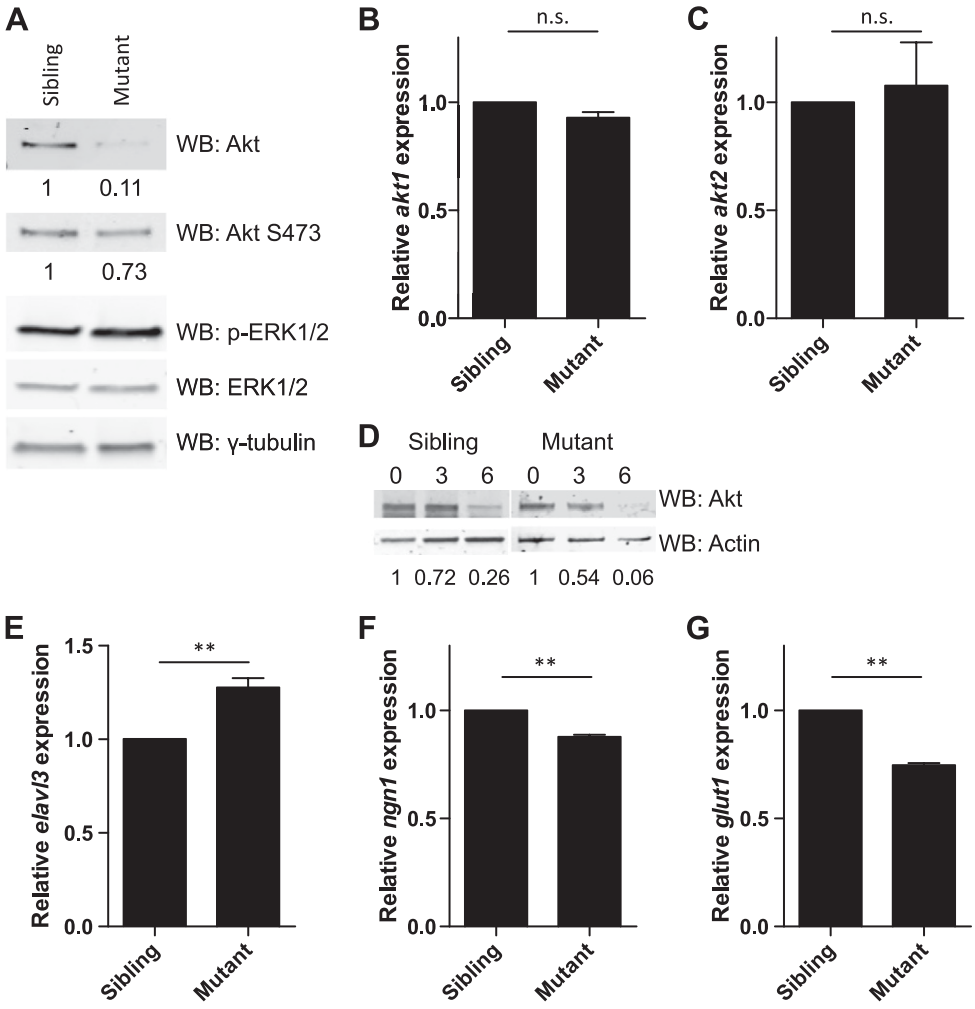

Figure 4. *cep55* homozygous mutants exhibit defects in PI3K/Akt pathway. Homozygous mutant and sibling 24 hpf embryos were analyzed by (*A*) Western blotting or (*B*, *C*, *E–G*) quantitative PCR for the indicated transcripts. Error bars represent SEM of 3 independent experiments. *D*) At 24 hpf, homozygous mutant and sibling embryos were treated with 100 μg/ml CHX for 0, 3, or 6 hours and analyzed by Western blotting. Quantification of Western blots was performed relative to γ-tubulin. n.s., not significant. $^{**}P < 0.01$

myr-Akt1 injection, and *myr-PIK3CA* injection. The embryos were assessed for rescue over several days.

Based on Mendelian genetics and prior experimental work, we predicted that one quarter of embryos resulting from the cross of 2 *cep55* heterozygous mutants should be homozygous mutants. Consistent with this, at 24 hpf we observed that 23.9% of uninjected fish exhibited a cloudy brain/eye and 26.0% were positive for acridine orange staining (**Fig. 5**). In contrast, only 12.4% of *myr-PIK3CA*-injected zebrafish exhibited a cloudy brain/eye and 12.7% were positive for acridine orange, indicating that PIK3CA was able to rescue approximately 50% of *cep55* homozygous mutants. Similarly, 16.1% of *myr-Akt1* injected zebrafish exhibited cloudy eye/brain and 17.4% were positive for acridine orange, indicating that AKT1 was able to rescue approximately 30% of *cep55* homozygous mutants. However, this effect was severely diminished by 48 hpf and gone by 72 hpf for both PIK3CA and AKT1.

We observed similar effects upon addition of the proteasome inhibitor, MG132 (Fig. 5; **Table 3**). Embryos were treated with 1 μM MG132 and assessed for rescue at 24 hpf. We observed 13.7% of MG132-treated zebrafish exhibited cloudy eye/brain and 14.6% were positive for acridine orange, indicating that MG132 was able to rescue *cep55* homozygous mutants to a similar degree as *myr-PIK3CA*. However, this effect was severely diminished by 48 hpf and gone by 72 hpf.

After analysis of gross morphology and acridine orange staining, we examined Akt levels in these groups by Western blotting. As expected, we could detect increased Akt levels following *myr-Akt1* mRNA injection; however, we also saw a clear increase in Akt levels upon both Pi3kca mRNA injection and MG132 treatment. Importantly, the amount of rescue corresponded with the change in Akt levels such that myr-AKT1, MG132, and myr-PIK3CA exhibited increasing levels of both Akt and rescue (Fig. 5; Table 3). These treatments also impacted upon Akt levels in normal embryos (Supplemental Fig. 3). Furthermore, myr-AKT1 exhibited less rescue than either myr-PIK3CA, which is upstream of Akt1 and Akt2, or MG132, which inhibits the proteasome thereby impacting upon global protein stability.

DISCUSSION

Analysis of cep55 homozygous mutants

Here we provide the first description of the role of Cep55 in embryonic development. ZfCep55 is 36% identical to hCEP55, with at least 2 of the 3 known phosphorylation sites conserved. This may indicate that the phosphorylation sites are used in zebrafish.

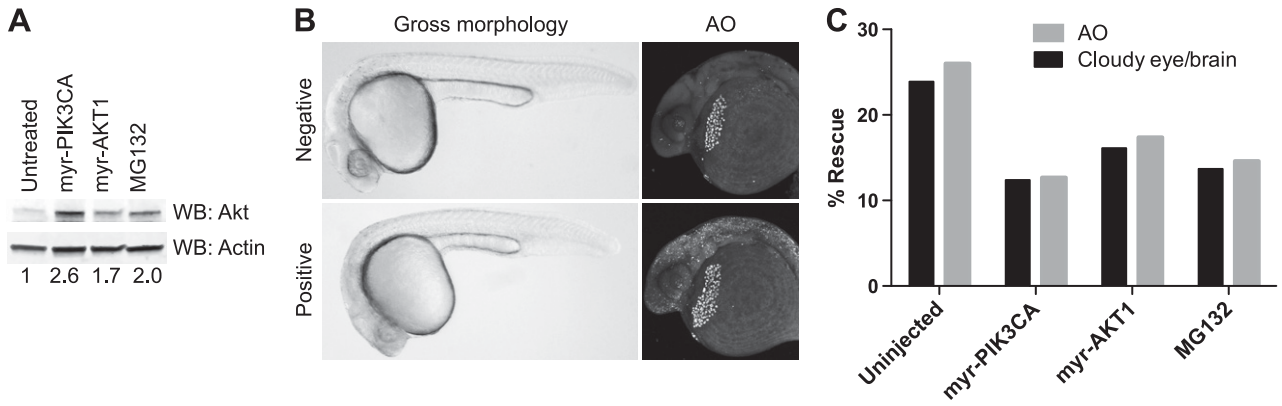

Figure 5. Injection of constitutively active *myr-PIK3CA* or *myr-Akt1* or treatment with MG132 can partially rescue the phenotype of homozygous mutants. Embryos were untreated, injected with *myr-PIK3CA* or *myr-AKT1* mRNA, or treated with 1 μM MG132. At 24 hpf the embryos were assessed for rescue as determined by gross morphology and AO staining. *A*) WB of Akt levels at 24 hpf after treatment. Quantification of WBs was performed relative to Actin. *B*) Representative images of positive and negative embryos. *C*) Graph of rescue as observed by gross morphology and AO staining at 24 hpf. AO, acridine orange; WB, Western blot.

Heterozygous mutants were both viable and fertile, suggesting that only 1 copy of *cep55* is required for embryonic development and gamete formation. Defects in homozygous mutants were first apparent at 24 hpf, with a cloudy eye and brain observed. Over time (24–72 h), defects became increasingly apparent in the hyperproliferative regions such as the brain and gut (36, 37), most likely as these regions are depleted of the maternal transcripts earlier than tissues that are not as proliferative (36). This suggests the role of Cep55 is not lineage-restricted.

Proliferation was impacted in the brain as homozygous mutants as they expressed less of the neuronal progenitor marker, *ngn1*, and more of the differentiated neuron marker, *elavl3*. This suggests that *cep55* homozygous mutants undergo premature differentiation, thereby impacting their ability to proliferate and promote cellularity.

At 24 hpf homozygous mutants exhibited a decrease in G1 concomitant with an increase in S, G2, and aneuploidy cells. Drug studies have revealed a role for AKT in S phase progression, although a direct link has not been shown. For example, treatment with either guggulsterone or epigallocatechin-3-gallate induces S phase arrest concomitant with suppression of AKT (38, 39). Hence, the S phase arrest may be due to the decrease in AKT stability. AKT is also known to promote G2/M transition, with expression of constitutively active AKT sufficient to overcome DNA damage-induced G2 arrest (40, 41). Furthermore, inhibition of the PI3K/AKT pathway or expression of dominant negative AKT results in G2/M arrest (41–44). Taken together, disruption of the PI3K/AKT pathway results in G2 arrest in some cell types, as observed in *cep55* homozygous mutants.

A role for Cep55 in cytokinesis during early embryonic development?

hCEP55 was initially identified as being essential for the completion of cytokinesis, with depleted cells exhibiting aneuploidy (1). Some aneuploidy was detected in *cep55* homozygous mutants by FACS at 24 hpf, but this was not sufficient to explain the increase in apoptosis observed at that time point.

The cytokinetic machinery is poorly understood in zebrafish with many of genes identified in other species not yet annotated or described. However, the cytokinesis

TABLE 3. *Quantitation of rescue as observed by gross morphology and AO staining at 24 hpf*

Phenotype rescue	Uninjected	myr-PIK3CA	myr-AKT1	MG132
Fish (*n*)	285	299	292	314
Expected ratio mutants to siblings	71 (214)	75 (224)	73 (219)	79 (235)
Cloudy eye per brain				
n	68	37	47	43
%	23.9	12.4	16.1	13.7
% Rescue	0	48.2	32.6	42.7
P	N/A	<0.001	0.022	0.002
AO+ve				
n	74	38	51	40
%	26.0	12.7	17.4	14.6
% Rescue	0	51.2	32.8	43.8
P	N/A	<0.001	0.015	<0.001

AO, acridine orange; +ve, positive.

defect in *cep55* homozygous mutants appears quite mild compared with other cytokinetic phenotypes described. For example, in zebrafish injection of dominant negative *mklp1*, which recruits Cep55 to the spindle midzone and midbody in preparation for cytokinesis (3), has been reported to impair cleavage, with approximately 30% of embryos failing to progress beyond the 4- to 8-cell stage (45). Similarly, homozygous mutation of *aurora B*, whose phosphorylation of Mklp1 is essential for normal cytokinesis (46), results in a lack of cellularization (47). In both situations, the developmental arrest occurred concomitant with an increase in multinucleation due to cytokinesis failure (45, 47). Although H&E staining of coronal sections at this time revealed a distinct lack of cellularity at 24 hpf, this likely represents a combination of massive apoptosis concomitant with premature neuronal differentiation similar to that observed in *akt1* morphant embryos (31), rather than cytokinesis failure.

Cep55 regulates the Pi3k/Akt pathway during early embryonic development

As observed here for *cep55* homozygous mutants, it has been shown that the cell death is *p53*-independent in *akt1* morphant embryos (31). Furthermore, PHH3 staining is unaffected in *akt1* morphant embryos. Neither the role of *p53* in cell death nor the effect of PHH3 staining has been tested in *akt2* morphant embryos.

Given that Pten inhibits the Akt pathway, *cep55* mutant zebrafish would be expected to exhibit the opposite phenotype to *pten* knockout. Zebrafish carry 2 copies of the *pten* gene, *ptena* and *ptenb*. Although homozygous null single mutants of either *pten* gene are viable and fertile, double homozygous null mutants exhibit enhanced cellular proliferation and reduced apoptosis (48), a phenotype opposite to *cep55* mutants. This evidence further implicates Cep55 as an activator of the PI3K/Akt pathway.

The duplication event that resulted in 3 *akt* genes occurred much earlier than the genome-wide duplication event that occurred in teleost fish resulting in co-orthologs for many genes as metazoans have 3 *akt* genes (49, 50). There is sufficient sequence variation and different modes of regulation to confer different functions to the *akt* orthologs (51). However, given the high level of sequence identity between proteins (~78% in zebrafish (26, 27)) it is not surprising homozygous *cep55* mutation results in the disruption of both Akt1- and Akt2-dependent pathways. We hypothesize that Akt3-dependent pathways would also be disrupted at later time points.

Cep55-dependent regulation of Akt was not due to a decrease in Akt1 or Akt2 transcription but a defect in Akt stability as determined by CHX chase and rescue by the proteasome inhibitor, MG132. This is in addition to known mechanisms in human cancer cell lines where the CEP55-PIK3CA interaction regulates AKT activation rather than stability (15, 16). Regardless of mechanism, Cep55-dependent regulation of either Akt stability or activation or both would have similar downstream consequences, as a reduction in Akt protein levels would limit the amount of activation. Further experiments are required to determine if CEP55 also regulates AKT stability during human embryonic development or in different contexts in cancer cells.

CEP55 was reported to be at the breakpoint in a patient with an Xp22/10q24 translocation (2). The patient had 3 copies of the CEP55 region and presented with a complex phenotype including motor retardation, agenesis of the corpus callosum, enlarged ventricles, diffuse reduction of white matter, facial dysmorphia, cleft lip and palate, and retinal pigment epithelium disturbance (2, 52). Although multiple genes may have been affected by this translocation, it is possible that at least a component of this phenotype is due to disruption of CEP55. Further analysis of patient samples to determine if PI3K/AKT signaling is hyperactivated may prove informative in determining the role of CEP55 in this phenotype.

Research by Chen *et al.* placed CEP55 and AKT as being downstream of VEGF-A in lung cancer (16). In contrast to the phenotype observed in *cep55* homozygous mutants, *vegf-a* morphant embryos exhibit an enlarged pericardium and blood vessel deficiencies (53). Overexpression studies have further described the role of Vegf-a in angiogenesis, vasculogenesis, and hematopoiesis (54). Although the cloudy eye/brain phenotype observed in *cep55* homozygous mutants is unlikely to occur due to suppression of a Vegf-a-dependent pathway, it may well still have a specific downstream function in Vegf-a-dependent endothelial cells. Further investigation is required to determine if Cep55 plays a role downstream of Vegf-a during later stages. Indeed, Pi3k/Akt signaling has been implicated in hematopoiesis and angiogenesis at later time points (55, 56).

In summary, our analysis of *cep55* homozygous mutants has provided important clues into the role of Cep55 in embryonic development. Based on the phenotype observed, we conclude that Cep55 plays a minor role in the regulation of cytokinesis during embryogenesis but its primary role is in the activation of the PI3K/Akt pathway during early development. Further investigation is required to determine how the contribution of Cep55 to the PI3K/Akt pathway is regulated during development. FJ

The authors thank Xiao Qing Chen and Jonathan Beesley for technical assistance. B.M.H. was supported by an Australian Research Council Future Fellowship (FT 011265). K.K.K. was supported by a National Health and Medical Research Council (NHMRC) Senior Principal Research Fellowship (ID: 613638; Australia). Part of the experiments were supported by the Australian Zebrafish Phenomics Facility (NHMRC Grant 455871).

REFERENCES

1. Fabbro, M., Zhou, B. B., Takahashi, M., Sarcevic, B., Lal, P., Graham, M. E., Gabrielli, B. G., Robinson, P. J., Nigg, E. A., Ono, Y., and Khanna, K. K. (2005) Cdk1/Erk2- and Plk1-dependent phosphorylation of a centrosome protein, Cep55, is required for its recruitment to midbody and cytokinesis. *Dev. Cell* **9**, 477–488
2. Martinez-Garay, I., Rustom, A., Gerdes, H. H., and Kutsche, K. (2006) The novel centrosomal associated protein CEP55 is present in the spindle midzone and the midbody. *Genomics* **87**, 243–253
3. Zhao, W.-M., Seki, A., and Fang, G. (2006) Cep55, a microtubule-bundling protein, associates with centralspindlin to control the midbody integrity and cell abscission during cytokinesis. *Mol. Biol. Cell* **17**, 3881–3896

4. Van der Horst, A., and Khanna, K. K. (2009) The peptidyl-prolyl isomerase Pin1 regulates cytokinesis through Cep55. *Cancer Res.* **69**, 6651–6659
5. Bastos, R. N., and Barr, F. A. (2010) Plk1 negatively regulates Cep55 recruitment to the midbody to ensure orderly abscission. *J. Cell Biol.* **191**, 751–760
6. Van der Horst, A., Simmons, J., and Khanna, K. K. (2009) Cep55 stabilization is required for normal execution of cytokinesis. *Cell Cycle* **8**, 3742–3749
7. Chang, Y.-C., Wu, C.-H., Yen, T.-C., and Ouyang, P. (2012) Centrosomal protein 55 (Cep55) stability is negatively regulated by p53 protein through Polo-like kinase 1 (Plk1). *J. Biol. Chem.* **287**, 4376–4385
8. Morita, E., Sandrin, V., Chung, H.-Y., Morham, S. G., Gygi, S. P., Rodesch, C. K., and Sundquist, W. I. (2007) Human ESCRT and ALIX proteins interact with proteins of the midbody and function in cytokinesis. *EMBO J.* **26**, 4215–4227
9. Lee, H. H., Elia, N., Ghirlando, R., Lippincott-Schwartz, J., and Hurley, J. H. (2008) Midbody targeting of the ESCRT machinery by a noncanonical coiled coil in CEP55. *Science* **322**, 576–580
10. Carlton, J. G., and Martin-Serrano, J. (2007) Parallels between cytokinesis and retroviral budding: a role for the ESCRT machinery. *Science* **316**, 1908–1912
11. Mondal, G., Rowley, M., Guidugli, L., Wu, J., Pankratz, V. S., and Couch, F. J. (2012) BRCA2 localization to the midbody by filamin A regulates cep55 signaling and completion of cytokinesis. *Dev. Cell* **23**, 137–152
12. Kuo, T. C., Chen, C. T., Baron, D., Onder, T. T., Loewer, S., Almeida, S., Weismann, C. M., Xu, P., Houghton, J. M., Gao, F. B., Daley, G. Q., and Doxsey, S. (2011) Midbody accumulation through evasion of autophagy contributes to cellular reprogramming and tumorigenicity. *Nat. Cell Biol.* **13**, 1214–1223
13. Pohl, C., and Jentsch, S. (2009) Midbody ring disposal by autophagy is a post-abscission event of cytokinesis. *Nat. Cell Biol.* **11**, 65–70
14. Ettinger, A. W., Wilsch-Bräuninger, M., Marzesco, A.-M., Bickle, M., Lohmann, A., Maliga, Z., Karbanová, J., Corbeil, D., Hyman, A. A., and Huttner, W. B. (2011) Proliferating versus differentiating stem and cancer cells exhibit distinct midbody-release behaviour. *Nat. Commun.* **2**, 503
15. Chen, C. H., Lu, P. J., Chen, Y. C., Fu, S. L., Wu, K. J., Tsou, A. P., Lee, Y. C. G., Lin, T. C. E., Hsu, S. L., Lin, W. J., Huang, C. Y. F., and Chou, C. K. (2007) FLJ10540-elicited cell transformation is through the activation of PI3-kinase/AKT pathway. *Oncogene* **26**, 4272–4283
16. Chen, C. H., Lai, J. M., Chou, T. Y., Chen, C. Y., Su, L. J., Lee, Y. C., Cheng, T. S., Hong, Y. R., Chou, C. K., Whang-Peng, J., Wu, Y. C., and Huang, C. Y. F. (2009) VEGFA upregulates FLJ10540 and modulates migration and invasion of lung cancer *via* PI3K/AKT pathway. *PLoS ONE* **4**, e5052
17. Inoda, S., Morita, R., Hirohashi, Y., Torigoe, T., Asanuma, H., Nakazawa, E., Nakatsugawa, M., Tamura, Y., Kamiguchi, K., Tsuruma, T., Terui, T., Ishitani, K., Hashino, S., Wang, Q., Greene, M. I., Hasegawa, T., Hirata, K., Asaka, M., and Sato, N. (2011) The feasibility of Cep55/c10orf3 derived peptide vaccine therapy for colorectal carcinoma. *Exp. Mol. Pathol.* **90**, 55–60
18. Martin, K. J., Patrick, D. R., Bissell, M. J., and Fournier, M. V. (2008) Prognostic breast cancer signature identified from 3D culture model accurately predicts clinical outcome across independent datasets. *PLoS ONE* **3**, e2994
19. Montero-Conde, C., Martín-Campos, J. M., Lerma, E., Gimenez, G., Martínez-Guitarte, J. L., Combalía, N., Montaner, D., Matías-Guiu, X., Dopazo, J., de Leiva, A., Robledo, M., and Mauricio, D. (2008) Molecular profiling related to poor prognosis in thyroid carcinoma. Combining gene expression data and biological information. *Oncogene* **27**, 1554–1561
20. Westerfield, M. (1993) *The Zebrafish Book: A Guide for the Laboratory Use of Zebrafish (Brachydanio rerio)*, University of Oregon Press, Eugene, Oregon
21. Kettleborough, R. N. W., Busch-Nentwich, E. M., Harvey, S. A., Dooley, C. M., de Bruijn, E., van Eeden, F., Sealy, I., White, R. J., Herd, C., Nijman, I. J., Fényes, F., Mehroke, S., Scahill, C., Gibbons, R., Wali, N., Carruthers, S., Hall, A., Yen, J., Cuppen, E., and Stemple, D. L. (2013) A systematic genome-wide analysis of zebrafish protein-coding gene function. *Nature* **496**, 494–497
22. Thisse, C., and Thisse, B. (2008) High-resolution in situ hybridization to whole-mount zebrafish embryos. *Nat. Protoc.* **3**, 59–69
23. Tucker, B., and Lardelli, M. (2007) A rapid apoptosis assay measuring relative acridine orange fluorescence in zebrafish embryos. *Zebrafish* **4**, 113–116
24. Shepard, J. L., Stern, H. M., Pfaff, K. L., and Amatruda, J. F. (2004) Analysis of the cell cycle in zebrafish embryos. In *Zebrafish: Cellular and Developmental Biology* (H. Detrich III, Northeastern University, Boston, MA, ed.), 76,109–125, Elsevier Academic Press, San Diego, California
25. Jeffery, J. M., Urquhart, A. J., Subramaniam, V. N., Parton, R. G., and Khanna, K. K. (2010) Centrobin regulates the assembly of functional mitotic spindles. *Oncogene* **29**, 2649–2658
26. Altschul, S. F., Madden, T. L., Schäffer, A. A., Zhang, J., Zhang, Z., Miller, W., and Lipman, D. J. (1997) Gapped BLAST and PSI-BLAST: a new generation of protein database search programs. *Nucleic Acids Res.* **25**, 3389–3402
27. Altschul, S. F., Wootton, J. C., Gertz, E. M., Agarwala, R., Morgulis, A., Schäffer, A. A., and Yu, Y.-K. (2005) Protein database searches using compositionally adjusted substitution matrices. *FEBS J.* **272**, 5101–5109
28. Cole, L. K., and Ross, L. S. (2001) Apoptosis in the developing zebrafish embryo. *Dev. Biol.* **240**, 123–142
29. Langheinrich, U., Hennen, E., Stott, G., and Vacun, G. (2002) Zebrafish as a model organism for the identification and characterization of drugs and genes affecting p53 signaling. *Curr. Biol.* **12**, 2023–2028
30. Fresno Vara, J. A., Casado, E., de Castro, J., Cejas, P., Belda-Iniesta, C., and González-Barón, M. (2004) PI3K/Akt signalling pathway and cancer. *Cancer Treat. Rev.* **30**, 193–204
31. Cheng, Y.-C., Hsieh, F.-Y., Chiang, M.-C., Scotting, P. J., Shih, H.-Y., Lin, S.-J., Wu, H.-L., and Lee, H.-T. (2013) Akt1 mediates neuronal differentiation in zebrafish *via* a reciprocal interaction with notch signaling. *PLoS ONE* **8**, e54262
32. Jensen, P. J., Gunter, L. B., and Carayannopoulos, M. O. (2010) Akt2 modulates glucose availability and downstream apoptotic pathways during development. *J. Biol. Chem.* **285**, 17673–17680
33. Shuang, C., Zhou, J.-F., Ling, L., Yun-Zhang, L., and Yun, L. (2011) Molecular cloning, expression and overexpression analysis of *AKT3* (PKBgamma) in zebrafish. *Acta Hydrobiologica Sinica* **35**, 717–726
34. Yeh, C.-M., Liu, Y.-C., Chang, C.-J., Lai, S.-L., Hsiao, C.-D., and Lee, S.-J. (2011) Ptenb mediates gastrulation cell movements *via* Cdc42/AKT1 in zebrafish. *PLoS ONE* **6**, e18702
35. Cheng, Y.-C., Scotting, P. J., Hsu, L.-S., Lin, S.-J., Shih, H.-Y., Hsieh, F.-Y., Wu, H.-L., Tsao, C.-L., and Shen, C.-J. (2013) Zebrafish rgs4 is essential for motility and axonogenesis mediated by Akt signaling. *Cell. Mol. Life Sci.* **70**, 935–950
36. Chakraborty, A., Uechi, T., Higa, S., Torihara, H., and Kenmochi, N. (2009) Loss of ribosomal protein L11 affects zebrafish embryonic development through a p53-dependent apoptotic response. *PLoS ONE* **4**, e4152
37. Wallace, K. N., Akhter, S., Smith, E. M., Lorent, K., and Pack, M. (2005) Intestinal growth and differentiation in zebrafish. *Mech. Dev.* **122**, 157–173
38. Shishodia, S., Sethi, G., Ahn, K. S., and Aggarwal, B. B. (2007) Guggulsterone inhibits tumor cell proliferation, induces S-phase arrest, and promotes apoptosis through activation of c-Jun N-terminal kinase, suppression of Akt pathway, and down-regulation of antiapoptotic gene products. *Biochem. Pharmacol.* **74**, 118–130
39. Shen, X., Zhang, Y., Feng, Y., Zhang, L., Xie, Y. -A., and Luo, X. Epigallocatechin-3-gallate inhibits cell growth, induces apoptosis and causes S phase arrest in hepatocellular carcinoma by suppressing the AKT pathway. *International Journal of Oncology*, **44**, 791–796
40. Kandel, E. S., Skeen, J., Majewski, N., Di Cristofano, A., Pandolfi, P. P., Feliciano, C. S., Gartel, A., and Hay, N. (2002) Activation of Akt/protein kinase B overcomes a G(2)/m cell cycle checkpoint induced by DNA damage. *Mol. Cell. Biol.* **22**, 7831–7841
41. Lee, S.-R., Park, J.-H., Park, E. K., Chung, C. H., Kang, S.-S., and Bang, O.-S. (2005) Akt-induced promotion of cell-cycle

progression at G2/M phase involves upregulation of NF-Y binding activity in PC12 cells. *J. Cell. Physiol.* **205**, 270–277
42. Ornelas, I. M., Silva, T. M., Fragel-Madeira, L., and Ventura, A. L. (2013) Inhibition of PI3K/Akt pathway impairs G2/M transition of cell cycle in late developing progenitors of the avian embryo retina. *PLoS ONE* **8**, e53517
43. Weir, N. M., Selvendiran, K., Kutala, V. K., Tong, L., Vishwanath, S., Rajaram, M., Tridandapani, S., Anant, S., and Kuppusamy, P. (2007) Curcumin induces G2/M arrest and apoptosis in cisplatin-resistant human ovarian cancer cells by modulating Akt and p38 MAPK. *Cancer Biol. Ther.* **6**, 178–184
44. Kuo, P.-L., Hsu, Y.-L., and Cho, C.-Y. (2006) Plumbagin induces G2-M arrest and autophagy by inhibiting the AKT/mammalian target of rapamycin pathway in breast cancer cells. *Mol. Cancer Ther.* **5**, 3209–3221
45. Chen, M.-C., Zhou, Y., and Detrich III, H. W. (2002) Zebrafish mitotic kinesin-like protein 1 (Mklp1) functions in embryonic cytokinesis. *Physiol. Genomics* **8**, 51–66
46. Guse, A., Mishima, M., and Glotzer, M. (2005) Phosphorylation of ZEN-4/MKLP1 by aurora B regulates completion of cytokinesis. *Curr. Biol.* **15**, 778–786
47. Yabe, T., Ge, X., Lindeman, R., Nair, S., Runke, G., Mullins, M. C., and Pelegri, F. (2009) The maternal-effect gene cellular island encodes aurora B kinase and is essential for furrow formation in the early zebrafish embryo. *PLoS Genet.* **5**, e1000518
48. Faucherre, A., Taylor, G. S., Overvoorde, J., Dixon, J. E., and Hertog, Jd. (2008) Zebrafish pten genes have overlapping and non-redundant functions in tumorigenesis and embryonic development. *Oncogene* **27**, 1079–1086
49. Scheid, M. P., and Woodgett, J. R. (2001) PKB/AKT: functional insights from genetic models. *Nat. Rev. Mol. Cell Biol.* **2**, 760–768
50. Taylor, J. S., Van de Peer, Y., Braasch, I., and Meyer, A. (2001) Comparative genomics provides evidence for an ancient genome duplication event in fish. *Philos. Trans. R. Soc. Lond. B Biol. Sci.* **356**, 1661–1679
51. Gonzalez, E., and McGraw, T. E. (2009) The Akt kinases: isoform specificity in metabolism and cancer. *Cell Cycle* **8**, 2502–2508
52. Martinez-Garay, I., Jablonka, S., Sutajova, M., Steuernagel, P., Gal, A., and Kutsche, K. (2002) A new gene family (FAM9) of low-copy repeats in Xp22.3 expressed exclusively in testis: implications for recombinations in this region. *Genomics* **80**, 259–267
53. Nasevicius, A., Larson, J., and Ekker, S. C. (2000) Distinct requirements for zebrafish angiogenesis revealed by a VEGF-A morphant. *Yeast* **17**, 294–301
54. Liang, D., Chang, J. R., Chin, A. J., Smith, A., Kelly, C., Weinberg, E. S., and Ge, R. (2001) The role of vascular endothelial growth factor (VEGF) in vasculogenesis, angiogenesis, and hematopoiesis in zebrafish development. *Mech. Dev.* **108**, 29–43
55. Liu, L., Zhu, S., Gong, Z., and Low, B. C. (2008) K-ras/PI3K-Akt signaling is essential for zebrafish hematopoiesis and angiogenesis. *PLoS ONE* **3**, e2850
56. Choorapoikayil, S., Kers, R., Herbomel, P., Kissa, K., and den Hertog, J. (2014) Pivotal role of Pten in the balance between proliferation and differentiation of hematopoietic stem cells in zebrafish. *Blood* **123**, 184–190

Received for publication September 29, 2014.
Accepted for publication January 5, 2015.